

Ghosting of Pulmonary Nodules with Respiratory Motion: Comparison of Helical and Conventional CT Using an In Vitro Pediatric Model

Gary D. Luker¹
Kyongtae T. Bae
Marilyn J. Siegel
Steven Don
James A. Brink
Ge Wang
Thomas F. Herman

OBJECTIVE. The study was designed to compare helical CT with varying pitch and reconstruction intervals and conventional CT for revealing pulmonary nodules in a model that simulates respiratory motion in children.

MATERIALS AND METHODS. CT scans were obtained in an experimental model with one nodule (3 or 10 mm) in each scan. One-second scans were obtained at rates of 10, 20, and 30 respirations per minute using conventional CT with 4-mm collimation and table incrementation and helical CT with 4-mm collimation and either 4-mm/sec (pitch, 1:1) or 8-mm/sec (pitch, 2:1) table speed. Reconstructions were at 1-, 2-, and 4-mm intervals for scans obtained using 4-mm/sec table speed and at 1- and 4-mm intervals for scans obtained using 8-mm/sec table speed. Images were independently reviewed by three radiologists who estimated the number of nodules on each image.

RESULTS. Ghosting (depiction of more than one nodule in a study) was seen in 79%, 80%, and 75% of helical CT scans obtained with a 1:1 pitch using 1-, 2-, and 4-mm reconstruction intervals, respectively. By comparison, ghosting was seen in only 54% and 58% of helical CT scans with a 2:1 pitch using 1-mm reconstruction intervals and 4-mm reconstruction intervals, respectively, and in 56% of conventional CT scans ($p < .0001$). A single nodule was detected on all other scans, and at least one nodule was seen on all scans.

CONCLUSION. Ghosting of nodules is common in this model. Ghosting was seen less often on conventional scans and helical scans with 2:1 pitch than it was on helical scans with 1:1 pitch. Nonetheless, ghosting was seen on more than 50% of all scans with each technique.

Previous studies of chest CT in adults have shown better detection of pulmonary nodules with helical CT than with conventional CT [1, 2]. In addition to increasing detection of nodules, helical CT has led to identification of more small nodules (≤ 0.5 cm) [1]. The improved detection of pulmonary nodules with helical CT results from scanning during a single breath-hold, eliminating the misregistration between contiguous slices that can occur with conventional CT. Detection of nodules and diagnostic confidence are also increased by overlapping reconstructions from the helical data set [3].

Unlike adults, many children cannot cooperate with commands to suspend respiration, so chest CT examinations on chil-

dren approximately 6 years old or less are typically performed during normal quiet respiration. As a result, slice misregistration artifacts can occur, even with helical CT examinations. Techniques have been described for performing chest CT with respiratory gating, but these methods are not routinely available for clinical use [4, 5]. Even ultrafast CT scans are unable to completely eliminate respiratory motion [6]. Although bronchiectasis and duplication of fissures have been described as artifacts resulting from respiratory motion, the effects of respiratory motion on detection of pulmonary nodules have not been investigated to our knowledge [7, 8]. The purposes of this study are to compare how well helical and conventional CT reveal pulmonary nodules in a model designed to simu-

Received March 14, 1996; accepted after revision May 7, 1996.

¹All authors: Mallinckrodt Institute of Radiology, Washington University School of Medicine, 510 S. Kingshighway Blvd., St. Louis, MO 63110. Address correspondence to M. J. Siegel.

AJR 1996;167:1189-1193

0361-803X/96/1675-1189

© American Roentgen Ray Society

late respiratory motion in children and to determine the effects of pitch and reconstruction interval when using helical CT to reveal nodules in this same model.

Materials and Methods

Motion Phantom

A closed cylindrical chamber with 10-cm inner diameter and a length of 30 cm was constructed of polyvinyl chloride. At one end of the cylinder was an attachment port for connecting it to a respirator. A 1-mm-thick flexible latex diaphragm (attenuation, 60 H) sealed off the opposite end of the chamber. When attached to a respirator, the diaphragm consistently moved 11 mm (10 respirations per minute), 13 mm (20 respirations per minute), or 15 mm (30 respirations per minute). The differences in displacement with increasing respiratory rate were caused by slight differences in the compliance of the diaphragm at a fixed stroke volume. Although the model simulates respiratory motion, it does not precisely duplicate respiration. The phantom does not simulate normal chest wall compliance, and a breathing child would not be expected to have the same diaphragmatic excursion with each respiration at a given rate.

For each respiratory rate, the diaphragm was at rest for 50% of the respiratory cycle. It moved from rest to maximum displacement in 33% of the cycle time and returned to rest in the remaining 17% of the cycle. For example, at a rate of 20 respirations per minute, one respiratory cycle lasted 3 sec; the diaphragm was at rest for 1.5 sec, moved to maximum displacement in 1 sec, and returned to rest in 0.5 sec. A constant respirator stroke volume of 700 ml was used throughout the study. To simulate pulmonary nodules, a garbanzo bean (10-mm diameter; attenuation, 130 H) and a coriander seed (3-mm diameter; attenuation, 145 H) were attached to the outside of the latex diaphragm. The nodules moved with the diaphragm during respiration. The materials were selected to approximate the attenuation of actual pulmonary nodules and to simulate nodules smaller or larger than the collimation used for scanning.

CT Technique

CT studies were done with one nodule attached to the center of the diaphragm per study. Scans were done at 10, 20, and 30 respirations per minute. These respiratory rates encompass the rates encountered in older children. For all scans, the phantom was oriented with respiratory motion aligned with table motion (z -axis). We directed nodule motion along the z -axis (direction of table movement) to maximize the effect of respiratory motion and simulate the actual motion of a nodule in a child.

For each combination of nodule size and respiratory rate, the phantom was scanned using the following CT techniques: helical CT with 4-mm collimation, 4-mm/sec table speed, and 1:1 pitch; helical CT with 4-mm collimation, 8-mm/sec table speed, and 2:1 pitch; and conventional CT with 4-mm collimation and table incrementation. Reconstructions were done at 1-, 2-, or 4-mm intervals for scans obtained with 4-mm collimation and 4-mm/sec table speed. Reconstructions were done at 1- or 4-mm intervals for scans obtained with 4-mm collimation and 8-mm/sec table speed. Overlapping reconstructions were used to increase longitudinal resolution and detection of pulmonary nodules with helical CT [3, 9-11]. Four-millimeter collimation was selected because it is frequently used for chest CT examinations in small children. Three scans were performed with each nodule at rates of 10, 20, and 30 respirations per minute. All scans began 3 cm beyond the resting position of the diaphragm and continued through the resting position of the diaphragm. The total scan time was 10 sec for the helical scans at 1:1 pitch, 5 sec for the helical scans at 2:1 pitch, and 40 sec for the conventional scans. We did not try to start scanning at any fixed point in the respiratory motion cycle. We believe that the random start of scanning in this model simulates clinical examinations in children because scanning is not begun at a specific phase of respiration.

All scans were obtained with a Somatom Plus S scanner (Siemens Medical Systems, Iselin, NJ). Conventional CT scans were done using 120 kVp, 210 mA, 1-sec scan time, 3-sec interscan delay,

and a standard reconstruction algorithm. Helical CT examinations were performed with 120 kVp, 210 mA, and one scan per 360° rotation of the scanner. All other parameters were the same for both scan techniques. Axial images from the helical data were reconstructed using 180° linear interpolation and a standard algorithm. With the software available on the CT scanner, a single coronal plane reconstruction through the center of the nodule was generated from each set of axial images. Although axial images are used for clinical evaluation of nodules, the coronal reconstruction was chosen to summarize depiction of respiratory motion along the z -axis for the reviewers. Images were photographed at a lung-window setting (center, -600 H; width, 1600 H).

Image Analysis

All coronal reconstructions were reviewed independently by three radiologists who were unaware of the CT technique, helical CT reconstruction interval, respiratory rate, and size and number of nodules. For each coronal reconstruction, the radiologists estimated the number of apparent nodules (Figs. 1 and 2). The maximum number of actual nodules for 10, 20, and 30 respirations per minute was 108 at each rate (six CT images [three helical scans at the 1:1 pitch, two helical scans at the 2:1 pitch, and one conventional scan] \times three scans at each respiratory rate \times two differently sized nodules \times three reviewers).

Predicted Number of Intersections

To determine the number of times the CT beam could intersect the nodule, the displacement path and distance of the moving diaphragm versus time were graphed for both 10 and 20 respirations per minute. The path of the collimated scan beam versus time was also plotted for conventional CT and both helical CT pitches. These graphs were superimposed to determine the number of predicted intersections between the CT scan beam and the moving nodule at different phases of the respiratory cycle (Fig. 3). The selection of multiple diaphragmatic positions reproduces the clinical setting, in which scanning can begin at any phase of respiration. Table 1 gives the mean and range

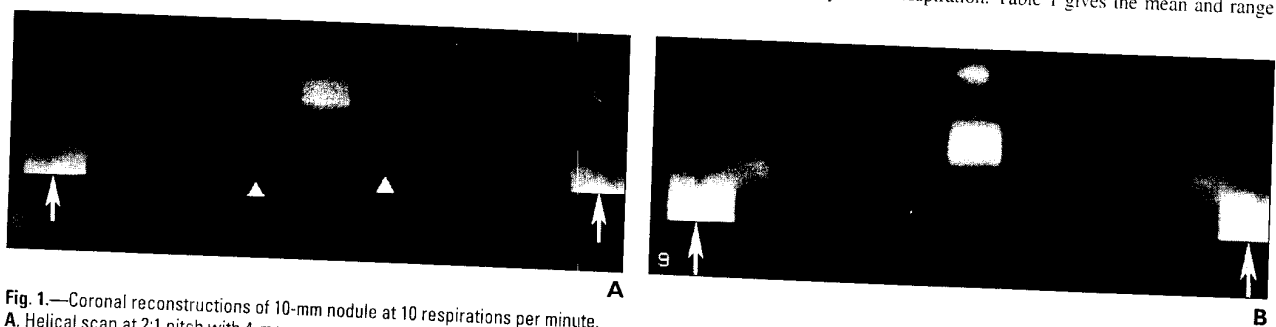


Fig. 1.—Coronal reconstructions of 10-mm nodule at 10 respirations per minute.
A. Helical scan at 2:1 pitch with 4-mm reconstruction intervals shows single nodule. All reviewers identified single nodule. Arrowheads = diaphragm.
B. Ghosting creates perception of two different nodules on conventional scan with 4-mm collimation and 4-mm table incrementation. All reviewers identified two nodules.
 Arrows = edges of cylinder.

CT of Pulmonary Nodule Ghosting

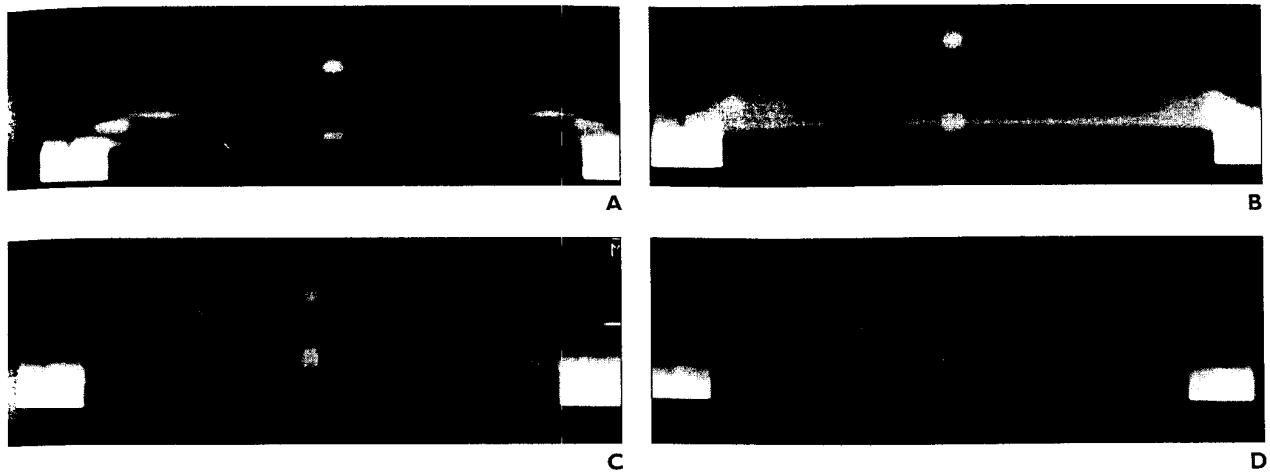


Fig. 2.—Coronal reconstructions of 3-mm nodule at 20 respirations per minute. **A–D,** Helical scan with 1:1 pitch and 1-mm reconstruction intervals (**A**), helical scan with 1:1 pitch and 4-mm reconstruction intervals (**B**), helical scan with 2:1 pitch and 1-mm reconstruction intervals (**C**), and conventional scan with 4-mm collimation and 4-mm table incrementation (**D**), show ghosting on all helical scans, with either two (**C**) or three (**A**) nodules estimated. Two reviewers detected two nodules and one reviewer perceived three nodules on **B**. All reviewers detected a single nodule on **D**.

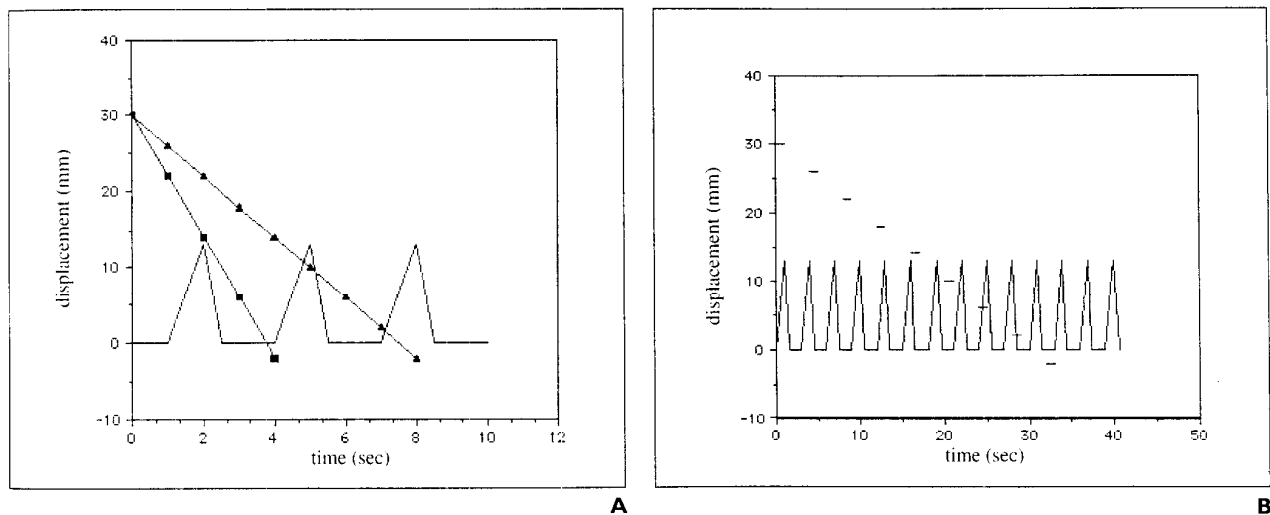


Fig. 3.—Predicted number of intersections at 20 respirations per minute. **A,** With helical CT, three intersections of CT beam and nodule moving with diaphragm (*straight line*) are seen using 1:1 pitch (*line with triangles*), compared with one intersection for 2:1 pitch (*line with squares*). **B,** With conventional CT, two intersections of CT beam and moving nodule are predicted. Interrupted horizontal lines = path of CT scan beam.

of intersections between the moving nodule and CT scan beam.

Statistical Analysis

Ghosting of nodules was defined as scans in which more than one nodule was identified. Absence of ghosting denoted scans in which only one nodule was detected, while images without a nodule were classified as no nodule. Differences in nodule depiction were analyzed for statistical significance using the chi-square test. Statistical significance was defined as $p < .05$ for all com-

parisons. Interobserver reliability in detection of nodules was analyzed with kappa statistics. Agreement using kappa statistics is reported as follows: .81–1.00 (perfect); .6–.8 (substantial); .4–.6 (moderate); .2–.4 (fair).

Results

At 30 respirations per minute, ghosting occurred on more than 96% of examinations, regardless of CT technique or nodule size. Because this respiratory rate yielded no

information about the other variables in this study, these data are not presented or analyzed further.

Table 2 shows the mean percentage of scans with ghosting for both nodule sizes and respiratory rates of 10 and 20 respirations per minute. When the results of both helical techniques and conventional CT were compared, ghosting was present on significantly fewer helical scans at 2:1 pitch and conventional scans (54–58%) than on

TABLE 1 Diaphragmatic Displacement and Predicted Number of Intersections Between the Diaphragm and the CT Scan Beam

Respirations per Minute	Diaphragmatic Displacement (mm)	Technique ^a	Pitch	No. of Intersections	
				Mean	Range
10	11	Helical	1:1	1.6	1-3
		Helical	2:1	1.1	1-2
20	13	Conventional		1.1	0-2
		Helical	1:1	2.6	2-3
		Helical	2:1	1.3	1-3
		Conventional		1.8	1-2

^aAll scans obtained with 4-mm collimation.

TABLE 2 Ghosting (Detection of More Than One Nodule per Scan) of 3-mm and 10-mm Nodules

Technique (Pitch)	Reconstruction Interval (mm)	Respirations per Minute	Mean ^a (%)	Nodule Size (%)		κ^a
				3-mm	10-mm	
Helical (1:1)	1	10	79	50	78	.74
		20		88	100	
	2	10	80	50	72	.84
		20		100	100	
Helical (2:1)	1	10	54 ^b	50	34 ^c	.96
		20		58 ^d	76	
	4	10	58 ^b	57	43 ^c	.78
		20		50 ^d	84	
Conventional	10	56 ^b	50	100	.7	
	20		50 ^d	25 ^e		

Note.—Helical scans were obtained with 4-mm collimation and 4-mm/sec (1:1 pitch) or 8-mm/sec (2:1 pitch) table speed. Conventional scans were obtained with 4-mm collimation and table incrementation.

^aBoth nodules and respiratory rates.

^bSignificantly less ghosting was present on helical scans at 2:1 pitch and conventional scans than on helical scans at 1:1 pitch ($p < .0001$).

^cAt 10 respirations per minute, significantly less ghosting of the 10-mm nodule was seen on helical scans at 2:1 pitch than on helical scans at 1:1 pitch and conventional scans ($p < .001$).

^dAt 20 respirations per minute, significantly less ghosting of the 3-mm nodule was seen on helical scans at 2:1 pitch and conventional scans than on helical scans at 1:1 pitch ($p < .001$).

^eAt 20 respirations per minute, significantly less ghosting of the 10-mm nodule was seen on conventional scans than on helical scans obtained with either pitch ($p < .0001$).

helical scans at 1:1 pitch (75–80%; Figs. 1 and 2). Differences in ghosting between scans with 2:1 pitch and conventional scans were not statistically significant ($p < .61$). The percentages of scans with ghosting using helical CT at 1:1 pitch also were not statistically different among the different reconstruction intervals ($p < .68$). Absence of ghosting was seen in the remaining scans with all CT techniques; at least one nodule was identified on every examination.

Mean percentages for ghosting of nodules are divided by nodule size and respiratory rate in Table 2. For the 3-mm nodule, ghosting was

identified in 50–57% of scans at 10 respirations per minute. The percentages of examinations with ghosting did not differ significantly among all CT techniques ($p < .69$). At 20 respirations per minute, ghosting of the 3-mm nodule occurred in 50–58% of studies with helical CT at 2:1 pitch and conventional CT. These percentages were significantly less than those for helical CT scans at 1:1 pitch (ghosting in 86–100%; $p < .001$). At 10 respirations per minute, ghosting of the 10-mm nodule was detected in 34% and 43% of examinations with helical CT at pitch 2:1 using 1- or 4-mm reconstruction intervals, respectively; these percent-

ages did not differ significantly ($p < .42$). Ghosting occurred on significantly fewer helical scans at 2:1 pitch of a 10-mm nodule at 10 respirations per minute than on helical scans at 1:1 pitch and conventional 4×4 scans ($p < .001$). With conventional CT, ghosting of the 10-mm nodule was seen on all examinations done at 10 respirations per minute. At 20 respirations per minute, the percentage of scans with ghosting of the 10-mm nodule on conventional CT (25%) was significantly less than the percentage with either helical CT technique (76–100%; $p < .0001$).

Interobserver agreement on the number of nodules was substantial or perfect for all CT techniques (Table 2). The lowest kappa value was .7 for conventional CT; the highest was .96 for helical CT with 1:1 pitch and 4-mm reconstruction intervals and helical scans with 2:1 pitch and 1-mm reconstruction intervals.

Discussion

The use of helical CT for the detection of pulmonary nodules has been reported in adult patients [1–3]. In adults, helical CT detects nodules better than conventional CT scanning does because it eliminates respiratory-induced slice misregistration. However, young children are usually unable to hold their breath for the CT examination. Respiratory motion artifacts result regardless of scan technique and may decrease diagnostic accuracy for detecting pulmonary nodules, particularly near the diaphragm, where respiratory motion is greatest [12]. Correct identification of numbers of pulmonary nodules is important because it has ramifications for tumor staging, choice of therapy, and evaluation of therapeutic regimens.

In this study, we designed a model to simulate pulmonary nodules moving with normal respiration. The data from this in vitro analysis show a significant overall difference in nodule depiction using conventional CT (4 mm collimation and table incrementation) and helical CT with 4-mm collimation and 8-mm/sec table speed (pitch, 2:1) compared with helical CT with 4-mm collimation and 4-mm/sec table speed (pitch, 1:1). At respiratory rates slightly lower than those observed in alert children but similar to the slower rates seen in mildly sedated patients (10–20 respirations per minute), ghosting of nodules was seen in 54%, 58%, and 56% of scans using helical CT with 2:1 pitch and 1- or 4-mm reconstruction intervals and conventional CT

CT of Pulmonary Nodule Ghosting

with 4-mm collimation and table incrementation, respectively. Ghosting was significantly more frequent with all helical scans obtained using a 1:1 pitch. For helical CT techniques, ghosting was independent of the reconstruction interval. Interobserver agreement for the number of nodules depicted was substantial or perfect for all scan techniques, regardless of the number of apparent nodules seen.

Ghosting occurs because the nodule is moving along the z -axis in both the positive and negative directions while the CT table is moving in the positive z -axis direction at a different rate. Because of this motion, the CT scan beam may intersect the nodule at more than one z -axis position, with the number of intersections increasing as the respiratory rate increases.

The differences in ghosting of nodules can be explained by the predicted number of different intersections between the moving diaphragm and the CT beam. For both respiratory rates, the predicted number of intersections was the greatest for helical CT with a 1:1 pitch; fewer intersections were predicted for conventional CT and helical CT with a 2:1 pitch (Table 1). For helical CT, ghost artifacts were seen less often at the 2:1 pitch than at the 1:1 pitch simply because the scan was completed more rapidly (5 sec for the 2:1 pitch versus 10 sec for the 1:1 pitch). Comparison of the conventional scans and the helical scans with a 1:1 pitch proves more interesting than comparison of different pitches on helical scans. The total scan time for conventional scans (40 sec) was much longer than that for helical scans obtained with a 1:1 pitch (10 sec). However, the scan beam was turned on for only 25% of the time (10 1-sec scans) with conventional CT. Although cases could be constructed in which the helical scans with a 1:1 pitch would intersect the nodule less times than conventional scanning does, the helical scan intersects the nodule more frequently on average with respect to the phase of respiration in our simulation. Because scanning was intermittent, fewer z -axis positions of the nodule were

detected with conventional CT scanning than with helical CT scanning using a 1:1 pitch. The data from the experimental model reflected the predicted number of intersections. Ghosting of the solitary nodule was observed with both conventional and helical CT scans, and indeed it occurred most frequently on helical CT scans at the 1:1 pitch.

The reviewers detected at least one nodule on all scans. For helical CT scans, this detection rate reflects the fact that the CT beam is activated throughout the scanning period, resulting in at least one intersection of the beam with the moving nodule. Conventional CT scans at 10 respirations per minute could fail to intersect a nodule because of discontinuous beam activation (Table 1), but we did not have this problem during the *in vitro* scanning with conventional CT.

Our model did not simulate bronchi and vessels found in the normal pulmonary parenchyma, which could affect *in vivo* depiction of nodules because scans done with helical CT at a 2:1 pitch increase the effective slice thickness by 30% compared with helical CT at a 1:1 pitch [13]. Broadening the effective slice profile will lead to increased volume averaging and decreased sharpness of edges of pulmonary nodules. Volume averaging with adjacent pulmonary parenchyma could worsen depiction of small nodules, despite the reduction in ghosting. However, anatomic landmarks could help the radiologist detect ghosting.

In conclusion, this *in vitro* analysis of respiratory motion and pulmonary nodule depiction shows that ghosting occurs with both helical and conventional CT techniques. Ghosting usually worsens with increasing respiratory rates. Helical CT scans using a 2:1 pitch or conventional CT scanning reduced ghosting compared with helical CT scans using a 1:1 pitch; however, ghosting is seen in more than 50% of examinations, regardless of scan technique. Our results suggest that using helical CT with a 2:1 pitch or conventional CT may improve depiction of pulmonary nodules in children. Further investigation with models that simulate more

than one nodule on a background of pulmonary parenchyma and studies in patients should be performed to confirm these data.

References

1. Remy-Jardin M, Remy J, Giraud F, Marquette CH. Pulmonary nodules: detection with thick-section spiral CT versus conventional CT. *Radiology* 1993;187:513-520
2. Costello P, Anderson W, Blume D. Pulmonary nodule: evaluation with spiral volumetric CT. *Radiology* 1991;179:875-876
3. Buckley JA, Scott WW, Siegelman SS, et al. Pulmonary nodules: effect of increased data sampling on detection with spiral CT and confidence in diagnosis. *Radiology* 1995;196:395-400
4. Mori M, Murata K, Takahashi M, et al. Accurate contiguous sections without breath-holding on chest CT: value of respiratory gating and ultrafast CT. *AJR* 1994;162:1057-1062
5. Ritchie CJ, Hsieh J, Gard MF, Godwin JD, Kim Y, Crawford CR. Predictive respiratory gating: a new method to reduce motion artifacts on CT scans. *Radiology* 1994;190:847-852
6. Ritchie CJ, Godwin JD, Crawford CR, Stanford W, Anno H, Kim Y. Minimum scan speeds for suppression of motion artifacts in CT. *Radiology* 1992;185:37-42
7. Mayo JR, Müller ML, Henkelman RM. The double-fissure sign: a motion artifact on thin-section CT scans. *Radiology* 1987;165:580-581
8. Tarver RD, Conces DJ, Godwin JD. Motion artifacts on CT simulate bronchiectasis. *AJR* 1988;151:1117-1119
9. Wang G, Vannier MW. Longitudinal resolution in volumetric x-ray CT: analytical comparison between conventional and helical CT. *Med Phys* 1994;21:429-433
10. Wang G, Brink JA, Vannier MW. Theoretical FWTM values in helical CT. *Med Phys* 1994;23:753-754
11. Kalendar WA, Placin A, Suss C. A comparison of conventional and spiral CT: an experimental study on detection of spherical lesions. *J Comput Assist Tomogr* 1994;18:167-176
12. Krudy AG, Doppman JL, Herdt JR. Failure to detect a 1.5 centimeter lung nodule by chest computed tomography. *J Comput Assist Tomogr* 1982;6:1178-1180
13. Polacin A, Kalendar WA, Marchal G. Evaluation of section sensitivity profiles and image noise in spiral CT. *Radiology* 1992;185:29-35